Electronic Supplementary Material (ESI) for Catalysis Science & Technology.

Supporting Information

Oxygen Reduction Reaction at $La_xCa_{1-x}MnO_3$ Nanostructures: Interplay between A-site Segregation and B-site Valency

*Verónica Celorrio, Laura Calvillo, Ellie Dann, Gaetano Granozzi, Ainara Aguadero, Denis Kramer, Andrea Russell, and David J. Fermín**

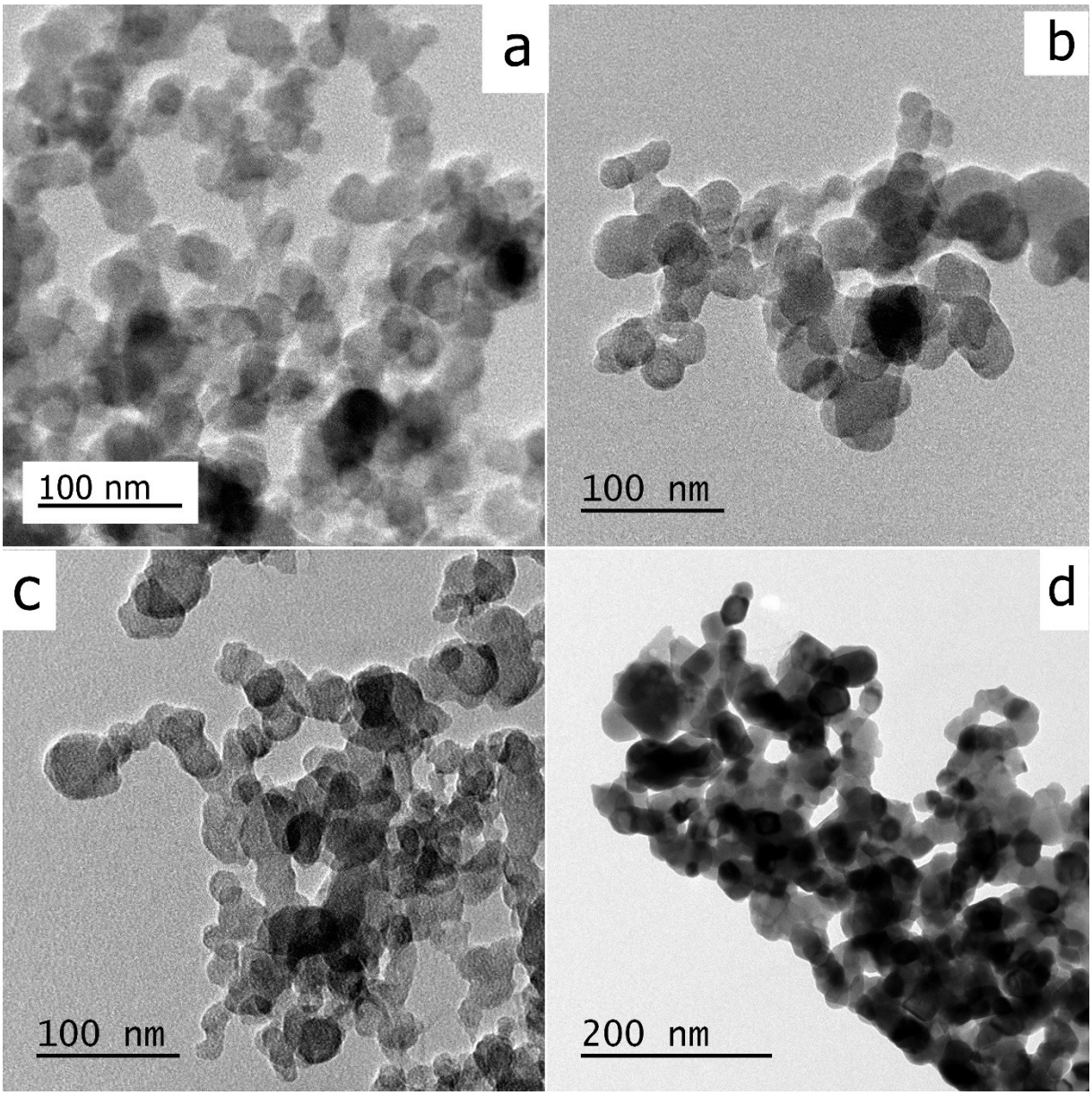

Figure S1. Characteristic TEM images of $CaMnO_3$ (a), $La_{0.37}Ca_{0.63}MnO_3$ (b) $La_{0.60}Ca_{0.40}MnO_3$ (c) and $LaMnO_3$ (d) oxide nanoparticles.

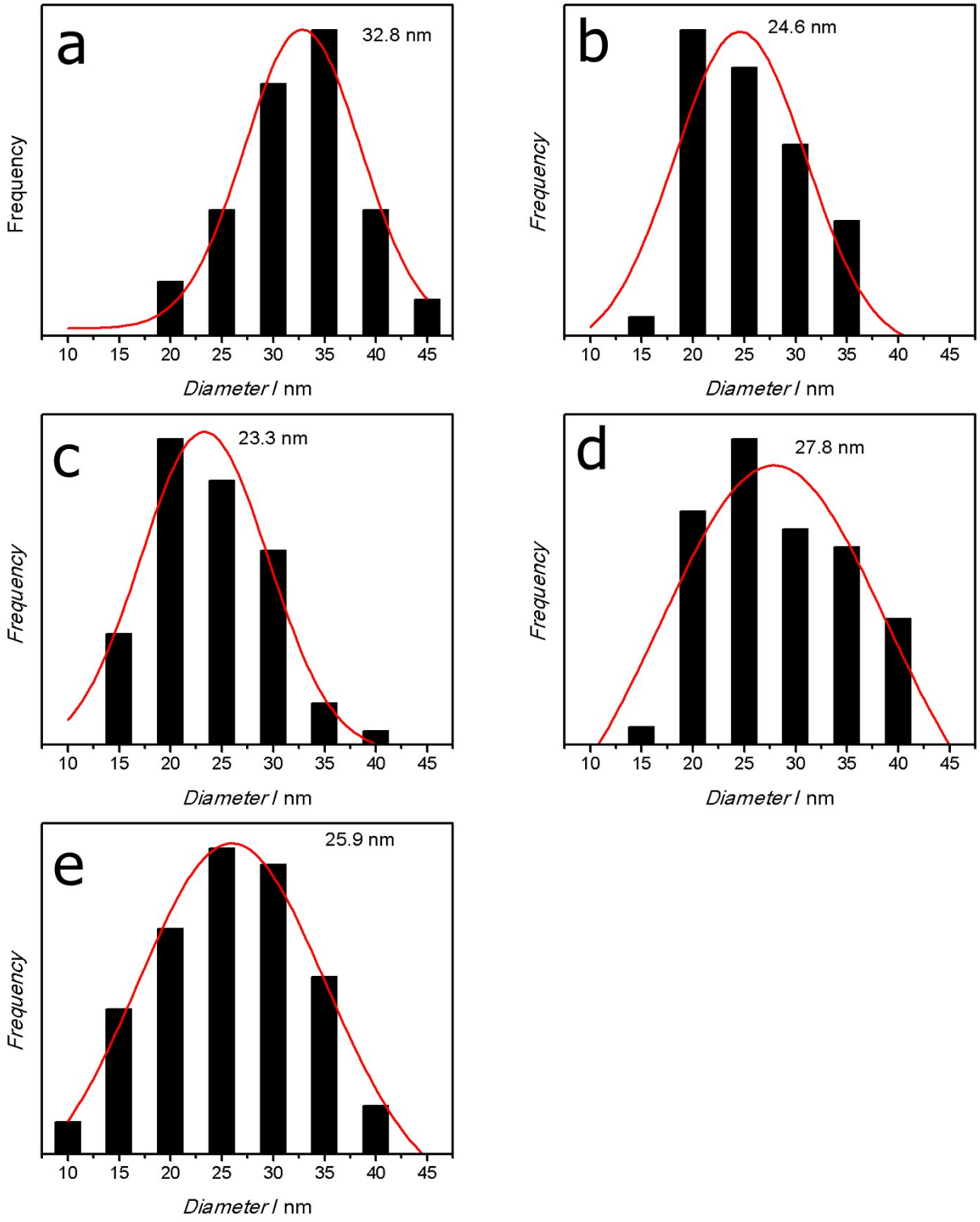

Figure S2. Particle size distributions obtained from TEM images of $LaMnO_3$ (a), $La_{0.81}Ca_{0.19}MnO_3$ (b), $La_{0.60}Ca_{0.40}MnO_3$ (c), $La_{0.37}Ca_{0.63}MnO_3$ (d) and $CaMnO_3$ (e) oxide nanoparticles. Mean nanoparticle diameters are indicated in the corresponding figures.

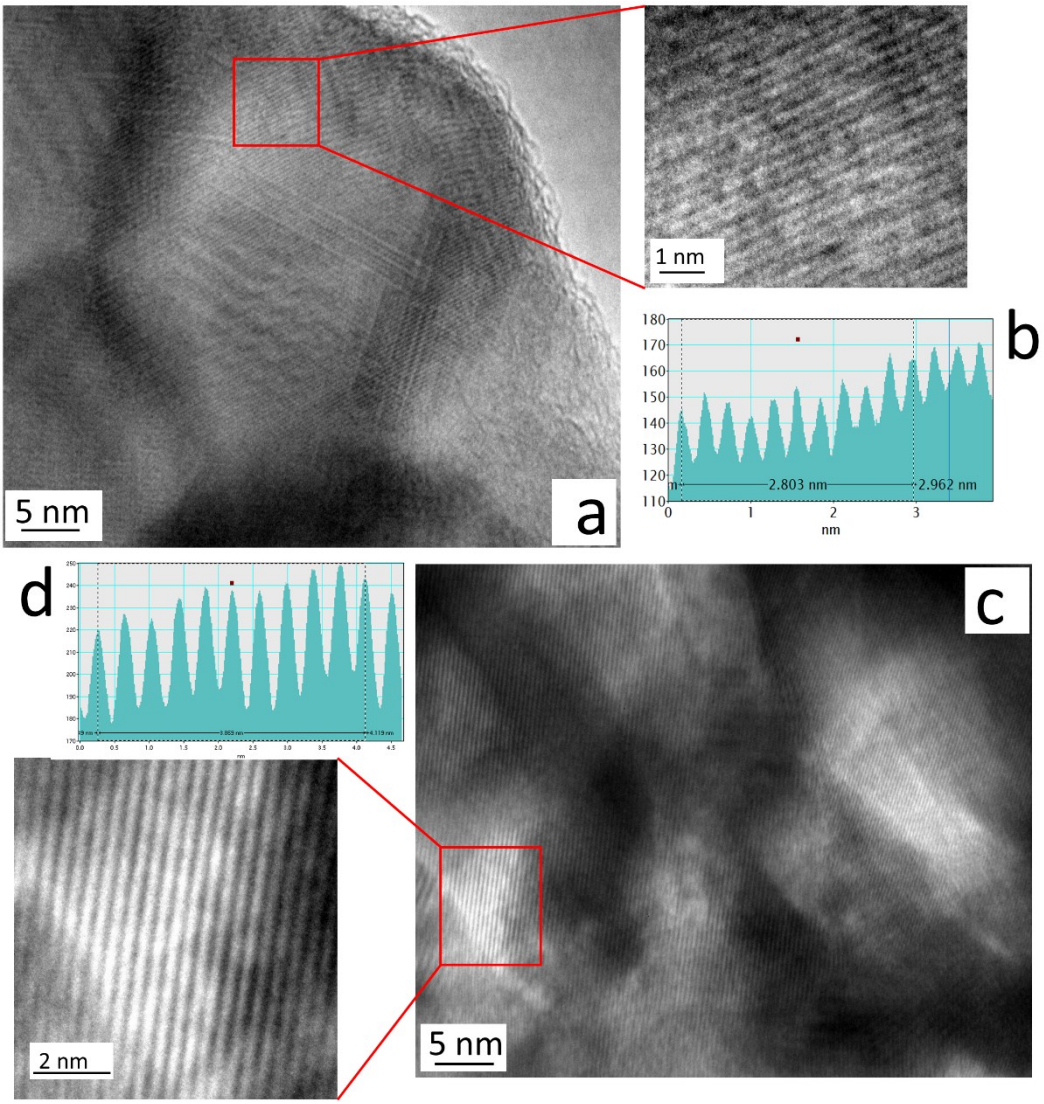

Figure S3. High resolution TEM images for $CaMnO_3$ (a) and $La_{0.81}Ca_{0.19}MnO_3$ (c) oxide nanoparticles. Figures b and d show the measured lattice spacing for $CaMnO_3$ (b) and $La_{0.81}Ca_{0.19}MnO_3$ (d). The distances between the planes equal 2.803 nm and 3.869 nm for CaMnO3 and $La_{0.81}Ca_{0.19}MnO_3$, respectively, ascribed to the {121} plane.

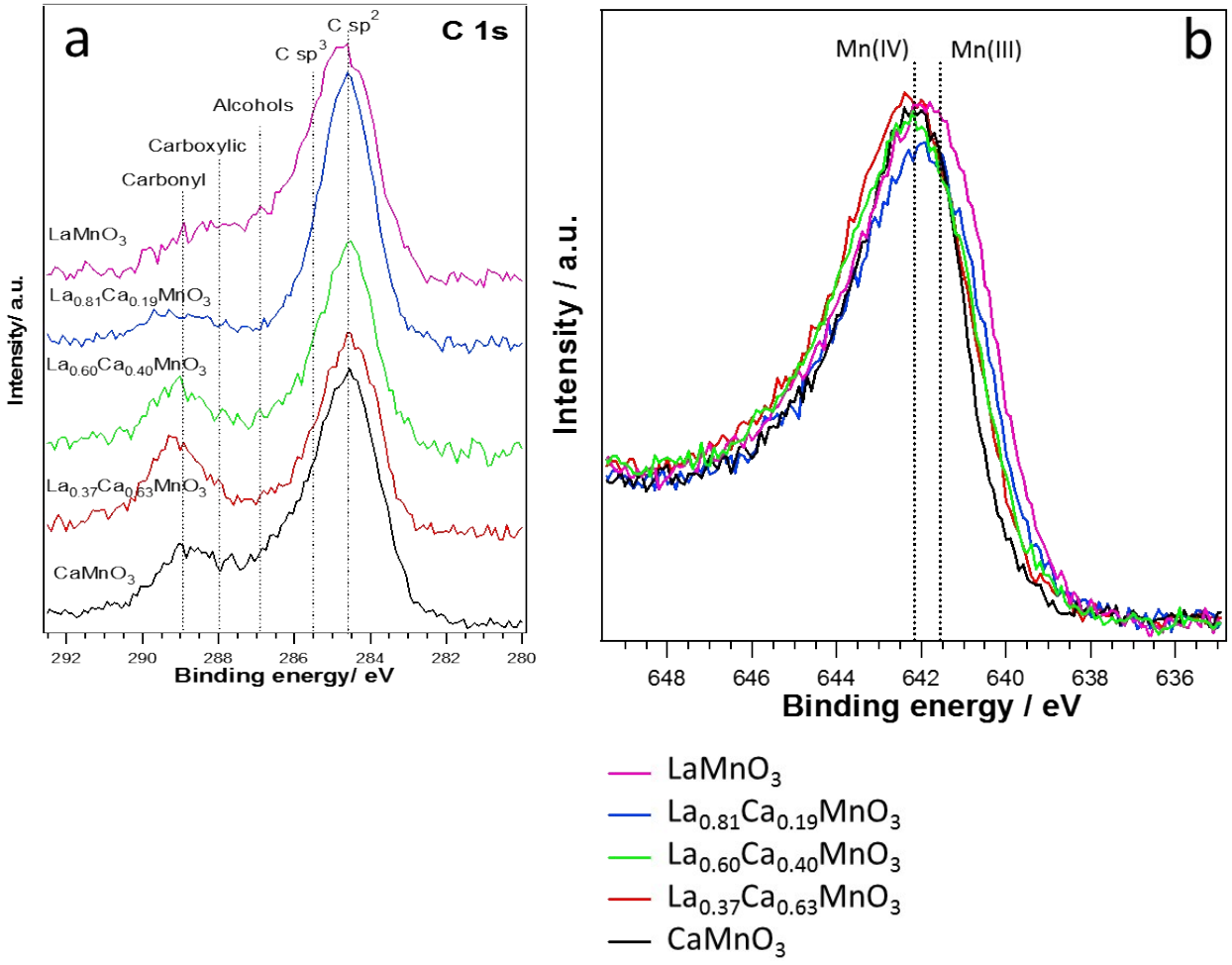

Figure S4. C 1s region (a) and enlargement of the Mn $2p_{3/2}$ peak (b) for the $La_xCa_{1-x}MnO_3$ samples. In Fig.S4b, it can be seen that there is a shift towards lower BE as *x* increases, indicating that the Mn^{3+}/Mn^{4+} ratio increases. This fact is in good agreement with the expected Mn^{4+} and Mn^{3+} oxidation states in the $CaMnO_3$ and $LaMnO_3$ samples, respectively.

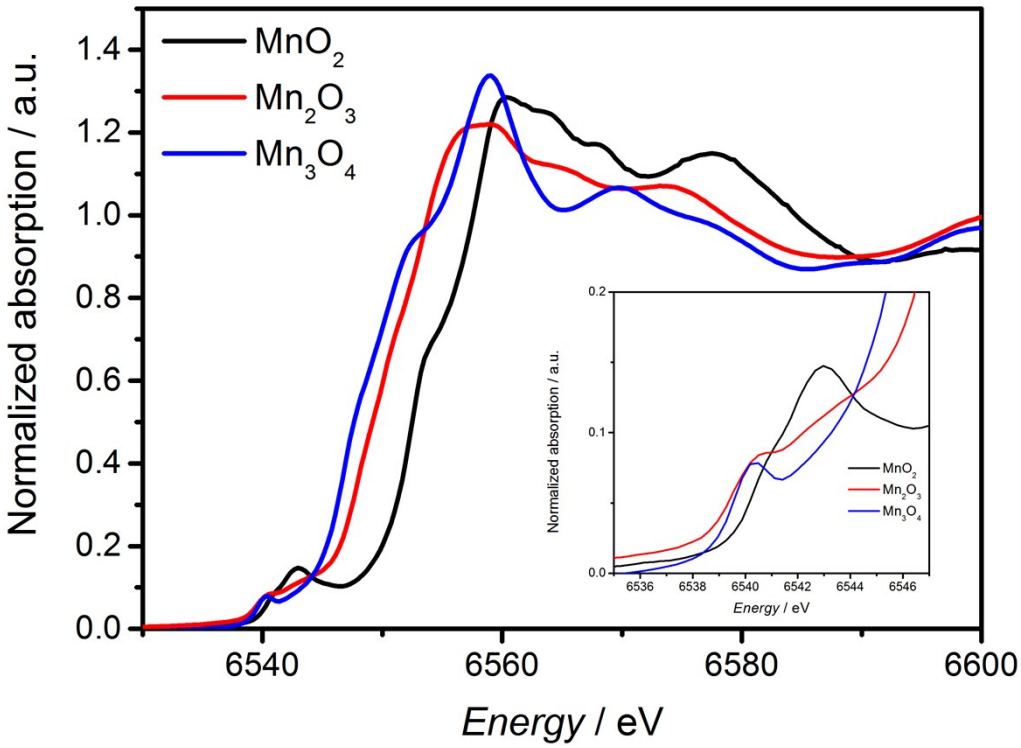

Figure S5. Normalised XANES spectra at the Mn K-edge of the standards Mn_3O_4, Mn_2O_3 and MnO_2 samples. The inset shows the pre-edge feature.

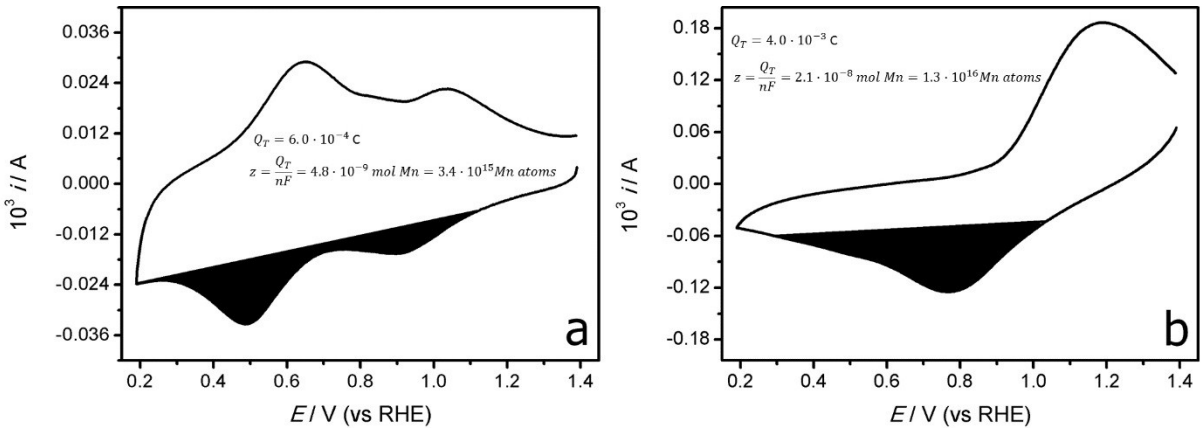

Figure S6. Calculation of the number of Mn atoms at the surface for $La_{0.81}Ca_{0.19}MnO_3$ (a) and $CaMnO_3$ (b) by integration of the cathodic responses employing a linear background subtraction. The number of electrons in the reduction process (*n*) per Mn atom is given by the difference in the initial oxidation state (estimated from XANES, Table S5) and the final oxidation state which correspond to Mn^{2+} in all cases.

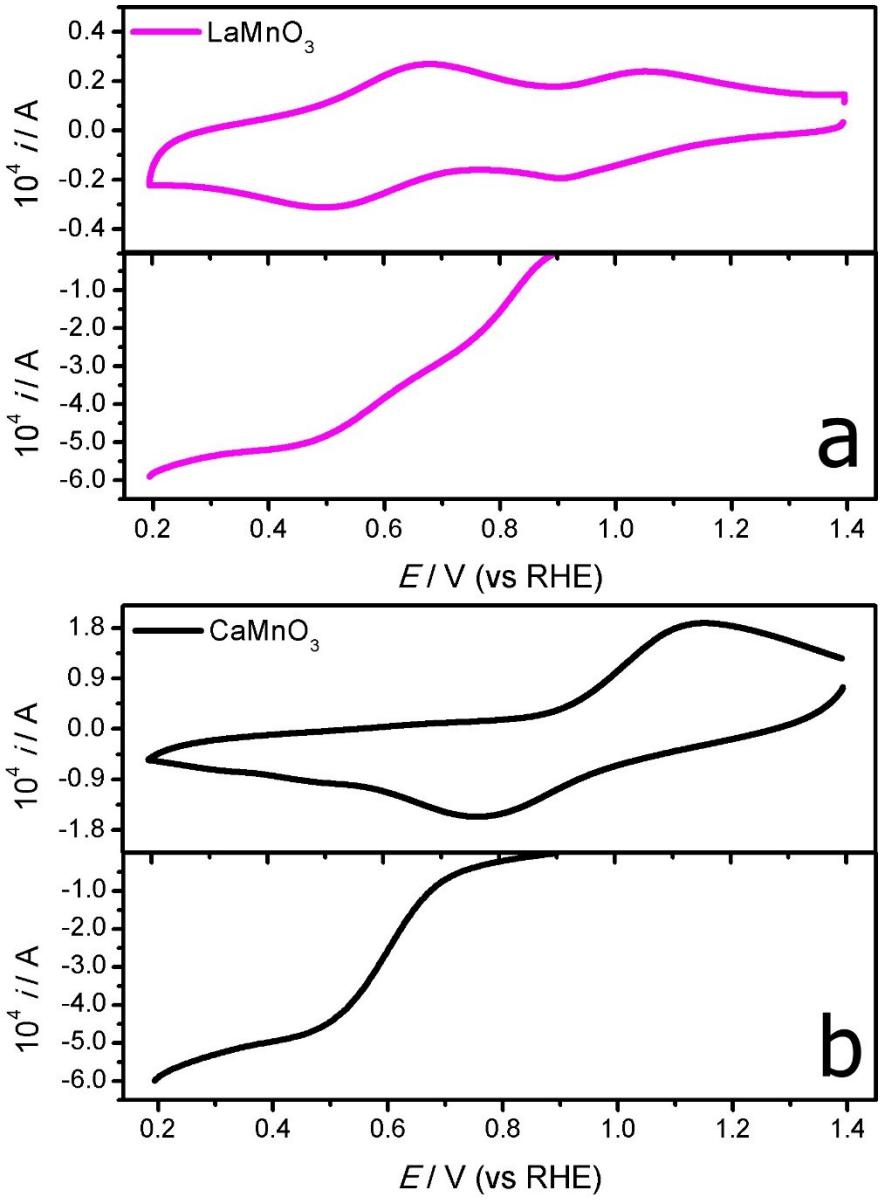

Figure S7. Overlay of the cyclic voltammograms measured in Ar-saturated 0.1 M KOH (top panels) and the disc current recorded at 1600 rpm in O_2-saturated 0.1 M KOH for $LaMnO_3$ (a) and $CaMnO_3$ (b) nanoparticles.

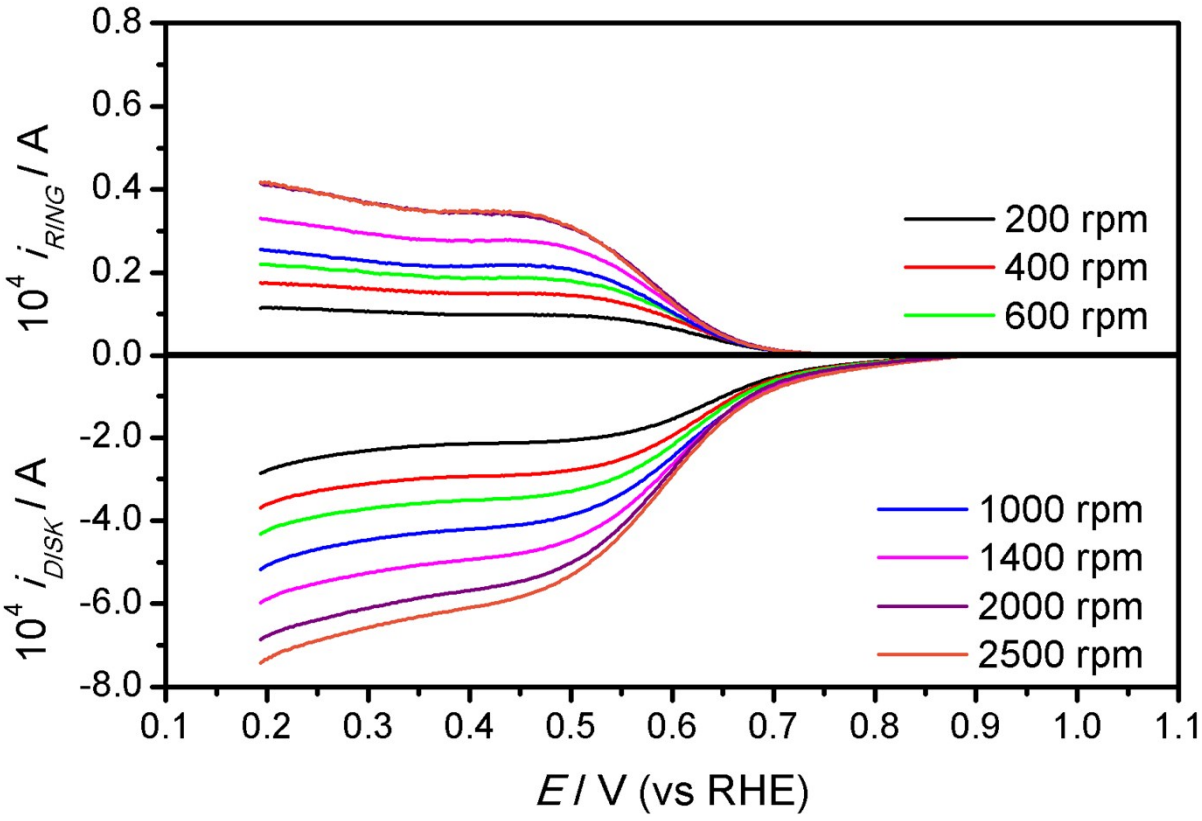

Figure S8. RRDE data of $CaMnO_3$ oxide nanoparticles at different rotation rates at 10 mV s^{-1}. The electrolyte was O_2-saturated containing 0.1 M KOH.

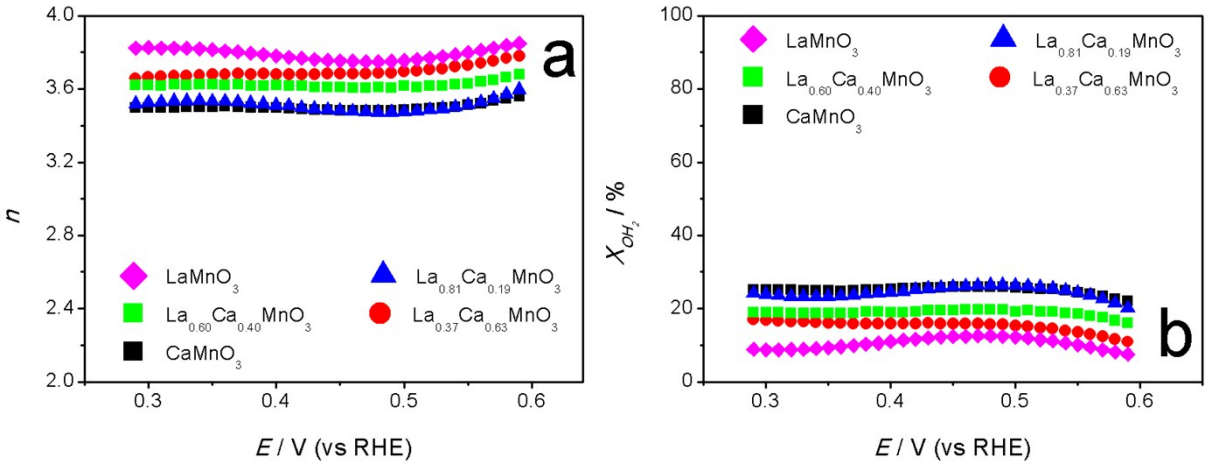

Figure S9. Number of electrons transferred, *n* (a) and HO_2^- yield (b) calculated from measurements of i_{RING} and i_{DISK} for $CaMnO_3$, $La_{0.34}Ca_{0.66}MnO_3$, $La_{0.5}Ca_{0.5}MnO_3$, $La_{0.67}Ca_{0.33}MnO_3$ and $LaMnO_3$ electrodes in O_2-saturated 0.1 M KOH at 1600 rpm. The potential range correspond to the diffusion limiting region. All of the catalysts mainly operates through the $4e^-$ process. The contributions to the peroxide formation are mostly related to thin mesoporous carbon layer.

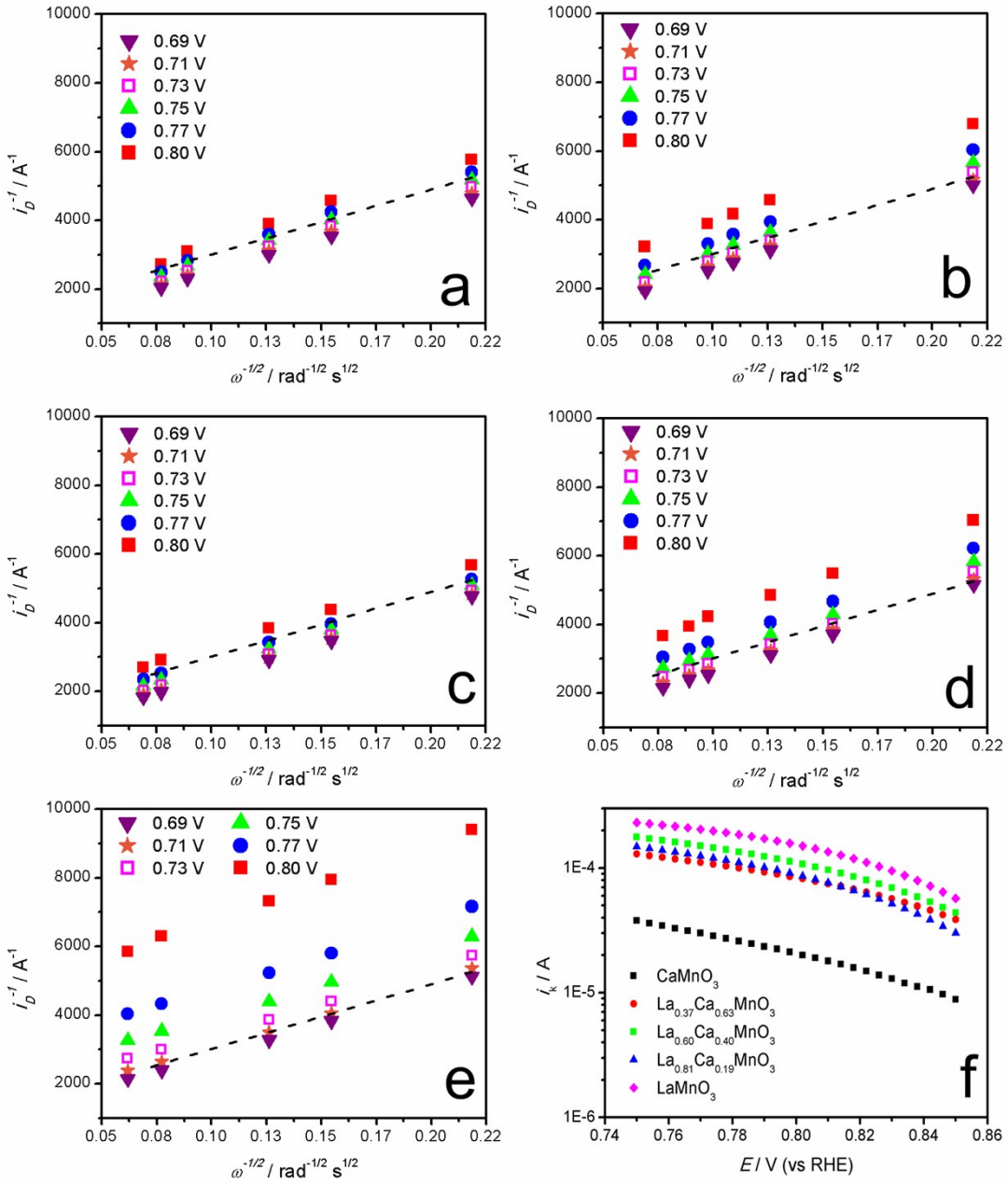

Figure S10. Koutecky-Levich plots for ORR at Vulcan supported $LaMnO_3$ (a), $La_{0.81}Ca_{0.19}MnO_3$ (b), $La_{0.60}Ca_{0.40}MnO_3$ (c), $La_{0.37}Ca_{0.63}MnO_3$ (d) and $CaMnO_3$ (e) nanoparticles in O_2-saturated 0.1 M KOH solution at different potentials. Dashed line shows the theoretical slope corresponding to the $4e^-$ ORR process (note this is not a fit to the data). Activities of the different catalysts at 10 mV s^{-1} calculated from the experimental data (f).

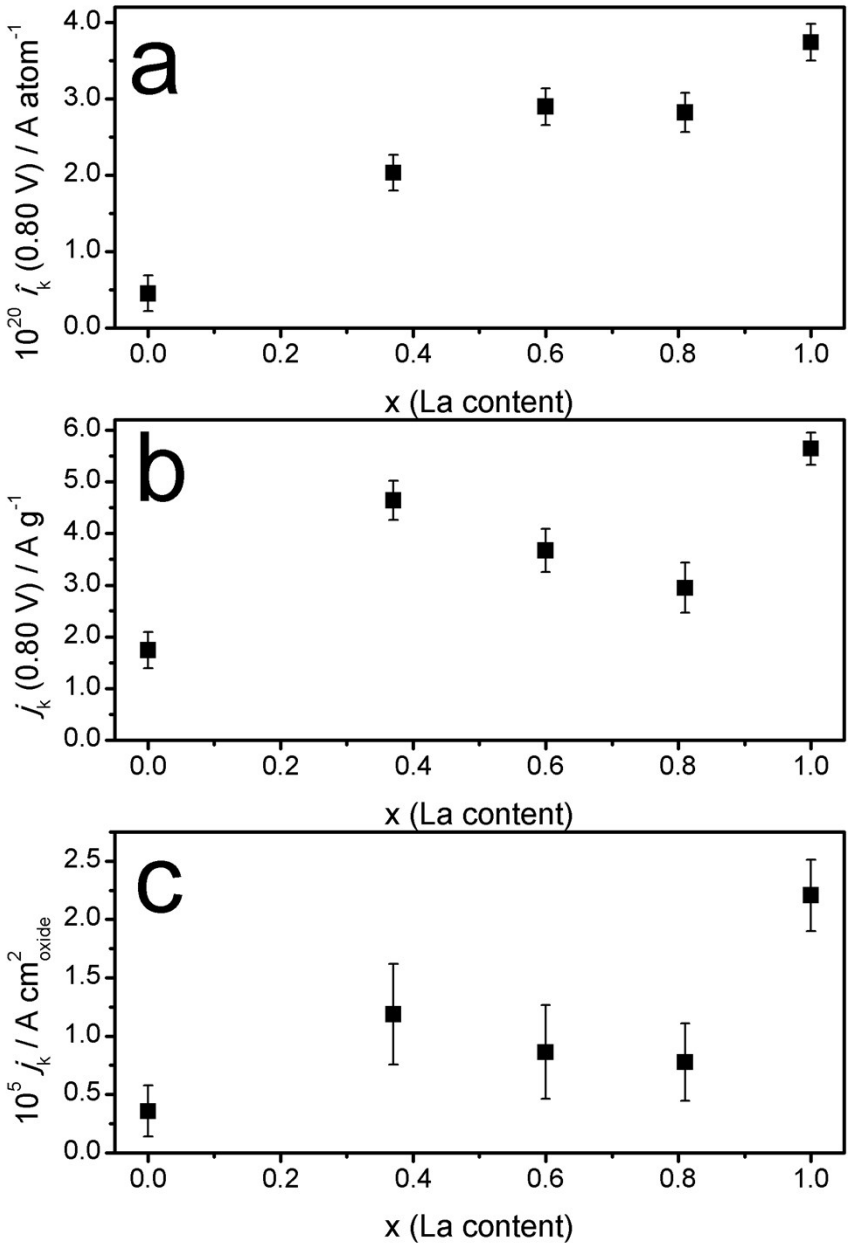

Figure S11. Kinetically limiting current at 0.80 V vs RHE normalised by the effective number of Mn atoms at the surface (a), mass of oxide at the electrode (b) and the area of oxide present at the electrode (c).

Table S1. Unit-cell parameters and statistics obtained from Rietveld refinement of the XRD patterns.

	$LaMnO_3$	$La_{0.81}Ca_{0.19}MnO_3$	$La_{0.60}Ca_{0.40}MnO_3$	$La_{0.37}Ca_{0.63}MnO_3$	$CaMnO_3$
Space Group	*Pm3m*	*Pnma*	*Pnma*	*Pnma*	*Pnma*
a [Å]	3.8873(3)	5.4553(6)	5.4230(4)	5.390(8)	5.2784(3)
b [Å]	---	7.696(2)	7.6522(11)	7.593(2)	7.4464(9)
c [Å]	---	5.441(2)	5.4484(9)	5.405(2)	5.2710(5)
La_{occ}	1.00	0.81(7)	0.60(2)	0.37(2)	---
Ca_{occ}	---	0.19(7)	0.40(2)	0.63(2)	1.00
Unit Cell Volume [$Å^3$]	58.74(7)	228.46(9)	226.098(5)	221.20(10)	207.20(3)
χ^2	3.21	2.76	1.22	2.97	1.36
R_p [%]	2.05	2.03	1.72	2.20	1.49
R_{wp} [%]	2.75	2.70	2.20	2.92	1.90
R_{exp} [%]	1.53	1.63	1.98	1.70	1.63
R_{Bragg} [%]	2.93	2.49	1.54	7.09	1.16

Table S2. Atomic composition of the various $La_xCa_{1-x}MnO_3$ samples obtained by Energy-dispersive X-ray spectroscopy (EDX-SEM). The Mn signal is used as reference.

	Composition (% Atomic)		
	La	Ca	Mn
$LaMnO_3$	1.05 ± 0.05	---	1.00
$La_{0.81}Ca_{0.19}MnO_3$	0.79 ± 0.02	0.20 ± 0.07	1.00
$La_{0.60}Ca_{0.40}MnO_3$	0.50 ± 0.09	0.50 ± 0.08	1.00
$La_{0.37}Ca_{0.63}MnO_3$	0.34 ± 0.04	0.66 ± 0.06	1.00
$CaMnO_3$	---	1.01 ± 0.02	1.00

Table S3. Density (ρ) obtained from XRD refinement and mean particle diameters (d) measured from TEM images of the various oxide nanoparticles materials. The specific surface area (SSA) was calculated assuming that the oxide nanoparticles are spherical,

SSA ($m^2\ g^{-1}$) = $6\times10^3/(\rho\times d)$

where d is the mean particle size determined by TEM (nm), and ρ is the theoretical density (g cm^{-3}).

	ρ / g cm^{-3}	d / nm	*SSA / $m^2\ g^{-1}$
$LaMnO_3$	6.81	32.8 ± 5.9	27.8 ± 7.1
$La_{0.81}Ca_{0.19}MnO_3$	6.27	24.6 ± 5.2	40.7 ± 12.3
$La_{0.60}Ca_{0.40}MnO_3$	5.65	23.3 ± 5.4	47.4 ± 14.4
$La_{0.37}Ca_{0.63}MnO_3$	5.40	27.8 ± 5.0	41.3 ± 10.5
$CaMnO_3$	4.59	25.9 ± 4.3	51.9 ± 12.2

*Note this calculation does not consider the so-called internal porosity of the materials.

Table S4. Analysis of the single chemical components of the Ca 2p region. For each single chemical component, the BE (eV) of the Ca $2p_{3/2}$ and amount (at. %) values are given. Peak 1 is assigned to lattice Ca, while peak 2 corresponds to CaO / $CaCO_3$.

	Peak	
	1	2
$CaMnO_3$	344.8 eV 64.4 %	346.7 eV 35.6 %
$La_{0.37}Ca_{0.63}MnO_3$	345.9 eV 63.4 %	347.2 eV 36.6 %
$La_{0.60}Ca_{0.40}MnO_3$	346.1 eV 63.2 %	347.2 eV 36.8 %
$La_{0.81}Ca_{0.19}MnO_3$	346.3 eV 58.6 %	347.4 eV 41.4 %

Table S5. Analysis of the single chemical components of the O 1s region. For each single chemical component, the BE (eV) and amount (at. %) values are given. Peak 1 is assigned to lattice oxygen, peak 2 to La_2O_3, peak 3 to hydroxyl species, peak 4 to carbonyl groups and $CaO/CaCO_3$ species, and peak 5 to adsorbed molecular water.

	Peak				
	1	2	3	4	5
$CaMnO_3$	528.5 eV 47.5 %	---	530.9 eV 27.1 %	532.0 eV 18.3 %	533.7 eV 7.1 %
$La_{0.37}Ca_{0.63}MnO_3$	528.5 eV 6.3 %	529.3 eV 47.1 %	531.1 eV 24.7 %	532.1 eV 13.4 %	533.1 eV 7.4 %
$La_{0.60}Ca_{0.40}MnO_3$	528.5 eV 5.4 %	529.3 eV 44.6 %	531.1 eV 22.5 %	532.1 eV 24.0 %	533.6 eV 3.5 %
$La_{0.81}Ca_{0.19}MnO_3$	528.5 eV 8.8 %	529.3 eV 50.3 %	531.2 eV 21.7 %	532.2 eV 16.3 %	533.7 eV 2.9 %
$LaMnO_3$	528.5 eV 5.4 %	529.2 eV 54.6 %	530.9 eV 22.1%	532.2 eV 11.2 %	533.7 eV 6.7 %

Table S6. A:B (A = La+Ca and B = Mn) and La:Ca atomic surface ratios for the various $La_xCa_{1-x}MnO_3$ samples as estimated by XPS.

	A : B	La : Ca
$LaMnO_3$	73 : 27	---
$La_{0.81}Ca_{0.19}MnO_3$	75 : 25	77 : 23
$La_{0.60}Ca_{0.40}MnO_3$	71 : 29	73 : 27
$La_{0.37}Ca_{0.63}MnO_3$	66 : 34	54 : 46
$CaMnO_3$	61 : 39	---

Table S7. Effective Mn oxidation state obtained by XANES, faradaic charge associated with the reduction of surface Mn sites, and effective number of Mn atoms at the electrocatalyst surface.

	Mn oxidation state	Charge / C	Mn atoms at the surface
$LaMnO_3$	2.803 ± 0.002	$(6.81\pm0.4)\times10^{-4}$	$(4.9 \pm 0.3)\times10^{15}$
$La_{0.81}Ca_{0.19}MnO_3$	3.175 ± 0.002	$(6.00\pm0.2)\times10^{-4}$	$(3.4 \pm 0.4)\times10^{15}$
$La_{0.60}Ca_{0.40}MnO_3$	3.515 ± 0.001	$(7.52\pm0.3)\times10^{-4}$	$(4.1 \pm 0.3)\times10^{15}$
$La_{0.37}Ca_{0.63}MnO_3$	3.699 ± 0.002	$(8.92\pm0.2)\times10^{-4}$	$(7.4 \pm 0.2)\times10^{15}$
$CaMnO_3$	4.008 ± 0.004	$(4.00\pm0.1)\times10^{-3}$	$(1.3 \pm 0.04)\times10^{16}$